Adaptable Robot Formation Control

Adaptive and Predictive Formation Control of Autonomous Vehicles

PHOTO COURTESY OF AUTHORS

By Audrey Guillet, Roland Lenain, Benoit Thuilot, and Philippe Martinet

The ability to use cooperative small vehicles is of interest in many applications. From material transportation to farming operations, the use of small machines achieving small tasks, but able to work together to complete larger tasks, permits us to rely on a unique kind of vehicle. To be efficient, such a point of view requires the vehicles to be, at least partially, autonomous and their motion must be accurately coordinated for the tasks to be properly achieved. This article proposes a control framework dedicated to the accurate control of a fleet of mobile robots operating in formation. Decentralized control relying on interrobot communication has been favored. To ensure a high relative positioning, adaptive and predictive control techniques are considered, allowing us to account for the influence of several phenomena (such as dynamic perturbations or bad grip conditions) depreciating the relevance of classical approaches based on ideal robots and ideal contact conditions assumptions.

Digital Object Identifier 10.1109/MRA.2013.2295946

Date of publication: 12 February 2014

Mobile Robot Cooperation

The recent progresses of mobile robotics in various contexts have been pointed out by the success of several teams in different challenges (such as those organized by the Defense

1070-9932/14/$31.00©2014IEEE

Advanced Research Projects Agency; see, for instance, [1] or [2]). Such examples demonstrate the capabilities of achieving autonomously driving tasks [3] in different contexts, making way for new services in many applications. From transportation systems [4], [5] to off-road robotics [6], automated mobile robots can help to improve people's everyday life.

If potentialities offered by a single automated robot are promising, the ability to control several robots in cooperation allows a high degree of adaptability and resource sharing, providing numerous opportunities. Beyond the research dedicated to numerous small robots control, investigated in swarm robotics (see [7]–[9]), the payload capability of several human-sized robots may be able to bring new solutions. For instance, in agriculture, the use of several light autonomous vehicles operating in formation, rather than a huge tractor, would allow farmers to reduce the environmental impact of their activities while preserving the level of production [10]. Fully autonomous formations or autonomous vehicles controlled with respect to a manually driven one, as shown in Figure 1 or developed in [11] and [12], could both be considered.

Several fields of robotic research must be gathered to address formation control [13], such as mobile robots localization, communication, environment perception, and so forth. In particular, to propose relevant systems able to meet social expectations (such as material transportation, area coverage for surveillance, agricultural applications, and so forth), the control of several mobile robots in various configurations must be generic enough to be applicable in different contexts. In addition, the mechanical properties of the robot, the terrain, the desired shape for the formation, and the robot's speed will vary and induce different phenomena, which have to be accounted for in outdoor applications. Whatever the work context, the control architecture should be able to preserve highly accurate relative positions servoing for the autonomous systems to be robust and reliable.

In this article, a general framework dedicated to adaptable robot formation control is proposed. It accounts for various kinds of dynamics encountered in a formation of several mobile robots (potentially heterogeneous), through an adaptive and predictive algorithm. Formation control is addressed from a path tracking point of view: a reference path is previously learned (by a manual driving or via path planning) or achieved online by the first vehicle driven manually. Then, the desired shape for the formation is defined with respect to the reference path, in terms of curvilinear distances between robots along the reference path and lateral deviations with respect to this trajectory. Robots localization data are exchanged via wireless communication, but control laws are computed locally: this allows us to take advantage of a supervised approach, limiting oscillating behaviors while permitting a necessary level of autonomy for each robot. Because of the adaptive and predictive approaches, highly accurate relative positioning may be obtained, whatever the path and the encountered dynamics and the variations in the desired formation shape. As a result, the control architecture proposed in this article constitutes a generic strategy for the formation control of mobile robots for various applications in different contexts.

The ability to control several robots in cooperation allows a high degree of adaptability and resource sharing.

Robot Formation Modeling for Motion Control

Extended Kinematic Model

In the proposed model shown in Figure 2, each robot is considered as a bicycle, i.e., a unique wheel stands for the front axle and another one for the rear one (standard Ackermann representation; see [14]). Nevertheless, in a practical case, the rolling without sliding assumption is not necessarily met. Robots can move on a ground with bad grip conditions (e.g., in off-road contexts) or the measured variables, such as the robot heading or the steering angle, may be biased due to poor calibration or indirect measurement. Rather than considering robust control approaches, an alternative may be to account for such perturbations within the model without requiring

Figure 1. A potential formation control application in agriculture.

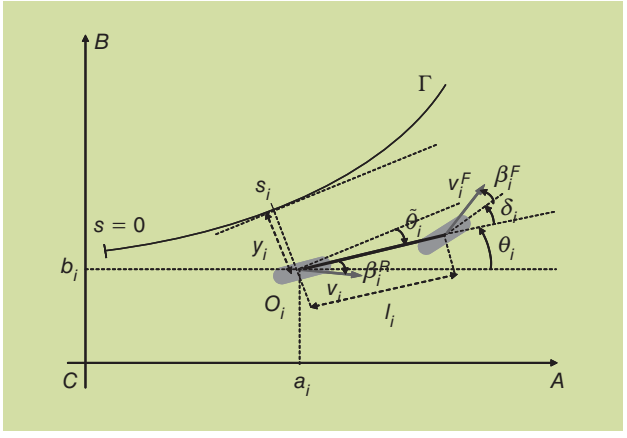

Figure 2. The extended kinematic model for formation control.

additional measured variables. More precisely, the proposed model differs from classical kinematic models in that two sideslip angles are considered, namely β^F and β^R for front and rear axles, respectively. These added variables are representative of the difference between the tire orientation and actual tire speed vector direction. Their estimation is discussed in the "Sideslip Angles Estimation" section. Longitudinal sliding has been neglected in this article, because of the low speed of the robots (around 2 m/s). This modeling approach offers two main advantages: 1) it allows us to avoid the use of complete dynamical models (such as those presented in [15]), hardly tractable since they require the knowledge of numerous parameters and 2) control design can still be derived by using the approaches proposed when rolling without sliding assumptions are valid.

The mission objectives, with the changes in the formation shape, have been achieved.

Based on these assumptions, two robot models are derived: 1) in a relative frame and 2) in an absolute one. In the "Robot Control" section, the parameters describing the formation shape are defined with respect to a common reference path. This path, made of a sequence of GPS points, can be previously planned or defined online by a first robot viewed as a leader.

Therefore, it is convenient to express the robot motion equations with respect to the reference path. The following notations, also depicted in Figure 2, are then introduced:

- Γ is the reference path used to specify the desired motion of the formation.
- O_i is the center of the ith mobile robot rear axle. It is the point to be controlled for each robot.
- s_i is the curvilinear coordinate of the closest point from O_i belonging to Γ. It corresponds to the distance covered along Γ by the ith robot.
- $c(s_i)$ denotes the curvature of path Γ at s_i.
- $\tilde{\theta}_i$ denotes the angular deviation of the ith robot with respect to Γ.
- y_i is the lateral deviation of the ith robot with respect to Γ.
- δ_i is the ith robot front wheel steering angle.
- l_i is the ith robot wheelbase.
- v_i is the ith robot linear velocity at point O_i.
- β_i^F and β_i^R denote the sideslip angles (front and rear) of the ith robot.

The motion equations for the ith mobile robot can then be expressed as (see [16] for details)

$$\begin{cases} \dot{s}_i = v_i \dfrac{\cos(\tilde{\theta}_i + \beta_i^R)}{1 - c(s_i) y_i} \\ \dot{y}_i = v_i \sin(\tilde{\theta}_i + \beta_i^R) \\ \dot{\tilde{\theta}}_i = v_i \left(\cos(\beta_i^R) \dfrac{\tan(\delta_i + \beta_i^F) - \tan(\beta_i^R)}{l_i} - \dfrac{c(s_i)\cos\tilde{\theta}_i}{1 - c(s_i) y_i} \right). \end{cases} \tag{1}$$

Equation (1) does not exist if $[1 - c(s_i) y_i] = 0$ (i.e., if point O_i is superposed with the instantaneous center of curvature of Γ). This situation is not encountered in practice however, since robots are supposed to be properly initialized.

The state vector $[s_i, y_i, \tilde{\theta}_i]^T$ of this first model is supposed to be measurable. Nevertheless, for a control law to be designed from model (1), the sideslip angles β_i^F and β_i^R have also to be available. As these variables cannot be easily measured, they have to be estimated by means of an observer. For reasons detailed below, the observer should preferably be designed from a robot model expressed in an absolute frame. The notations listed above are therefore supplemented with the following ones, also depicted in Figure 2:

- $[C, \vec{A}, \vec{B}]$ is an absolute reference frame
- (a_i, b_i) are the coordinates in the absolute frame of O_i, center of the ith mobile robot rear axle
- θ_i denotes the heading of the ith robot with respect to $\vec{A}$.

The motion equations for the ith mobile robot expressed in the absolute frame $[C, \vec{A}, \vec{B}]$ are derived from basic geometric considerations

$$\begin{cases} \dot{a}_i = v_i \cos(\theta_i + \beta_i^R) \\ \dot{b}_i = v_i \sin(\theta_i + \beta_i^R) \\ \dot{\theta}_i = v_i \cos(\beta_i^R) \dfrac{\tan(\delta_i + \beta_i^F) - \tan(\beta_i^R)}{l_i}. \end{cases} \tag{2}$$

Sideslip Angles Estimation

Both extended kinematic models (1) and (2) can be used to design a sideslip angles observer. In [17], model (1) is considered and the observer is built relying on the duality principle between observation and control. More precisely, this model is regarded as a process whose inputs are the sideslip angles β_i^F and β_i^R, and a control law is designed for these two variables to impose that the lateral and angular deviations $\hat{y}_i$ and $\hat{\tilde{\theta}}_i$, computed from model (1), converge to the corresponding measurements $\bar{y}_i$ and $\bar{\tilde{\theta}}_i$. Such a convergence ensures that model (1) is representative of the actual behavior of the vehicle whatever the grip conditions and sensor biases.

However, this observer presents two limitations. First, since the robot velocity v_i appears as a factor in the three equations in model (1), the observer is necessarily singular when $v_i = 0$. As a consequence, from a practical point of view, it has to be frozen when v_i is lower than an arbitrary threshold. When v_i increases and crosses the threshold, the observer is restarted, but transient inaccuracies in the sideslip angles estimation are likely to occur and may be detrimental to guidance accuracy. Next, if the reference trajectory is not an admissible path for the robots in some places (this may happen, due to noisy measurements, when Γ is built online from the data recorded by the leader robot), then the deviations $\bar{y}_i$ and $\bar{\tilde{\theta}}_i$ measured at these places by the ith robot present abrupt variations. These are erroneously interpreted as a sudden sliding phenomenon by the observer and an inaccurate sideslip angle estimation, detrimental to the guidance accuracy, may be returned.

Both limitations originate from the fact that the sliding effects are not estimated from the robot ego motion, but are estimated from its relative motion with respect to a reference trajectory. Therefore, an alternative observer is eventually proposed, designed from robot motion equations expressed in an absolute reference frame. The following observer derived from model (2) is considered

$$\begin{cases} \dot{\hat{\xi}}_i^p = f(\xi_i^p, \hat{\xi}_i^\beta, \delta_i, v_i) + \alpha_i^p(\tilde{\xi}_i^p) \\ \dot{\hat{\xi}}_i^\beta = \alpha_i^\beta(\xi_i^p, \tilde{\xi}_i^p \hat{\xi}_i^\beta, \delta_i, v_i), \end{cases} \tag{3}$$

where

- ξ_i^p is the state vector of model (2): $\xi_i^p = [a_i, b_i, \theta_i]^T$
- $\hat{\xi}_i^p$ and $\tilde{\xi}_i^p$ are respectively the associated observed state and observation error (i.e., $\tilde{\xi}_i^p = \hat{\xi}_i^p - \xi_i^p$, since the state vector ξ_i^p is supposed to be measurable)
- $\hat{\xi}_i^\beta$ is the sideslip angles estimation: $\hat{\xi}_i^\beta = [\hat{\beta}_i^F, \hat{\beta}_i^R]^T$
- $f(.)$ is the robot model, i.e., the right-hand term in (2)
- $\alpha_i^p(.)$ and $\alpha_i^\beta(.)$ are nonlinear functions designed to ensure that $(\tilde{\xi}_i^p)^T \tilde{\xi}_i^p + (\tilde{\xi}_i^\beta)^T \tilde{\xi}_i^\beta$ is a Lyapunov function (i.e., its derivative is negative), and moreover that $\tilde{\xi}_i^\beta$ converges to 0, so that $\hat{\xi}_i^\beta$ can be considered as a relevant estimation of the sideslip angles of the ith robot.

This alternative observer supplies relevant and reliable sideslip angle values that can be reported into the mobile robot model (1) to be accounted into the adaptive control law designed from such a model in the forthcoming section. With respect to classical localization devices used for mobile robot navigation, no complementary measurement is required.

Robot Control

Since all the variables appearing in model (1) are either measured (the localization sensors supplying the robot state vector $[s_i, y_i, \tilde{\theta}_i]^T$ are described in the "Experimental Testbed" section) or estimated (namely sideslip angles, see the "Sideslip Angles Estimation" section), accurate motion control of the robots formation can be addressed.

For each robot, the set points are defined with respect to the common reference trajectory Γ, provided beforehand or built online as the first robot is moving. More precisely, the objective for the ith robot (see Figure 3) is to track the path Γ with

- a desired lateral deviation y_i^d
- a desired curvilinear distance d_i^k with respect to the kth robot (d_i^k is evaluated along Γ and therefore remains perfectly consistent whatever the curvature of Γ).

A fixed formation shape is specified by constant set points. For instance, a wing-shaped formation is imposed in Figure 3 since

$$\begin{aligned} &y_1^d = 0 \quad y_2^d = y^* \quad y_3^d = 2y^* \quad \cdots \\ &d_2^1 = d^* \quad d_3^1 = 2d^* \quad \cdots. \end{aligned}$$

Alternatively, a regular platoon shape can be specified [see Figure 4(a)], by choosing

$$y_i^d = 0 \quad d_i^1 = (i-1)d^* \quad \forall_i \epsilon \{1, ..., n\}.$$

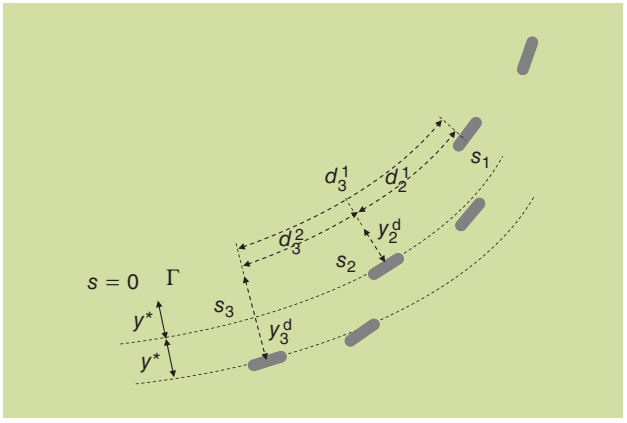

Figure 3. The set points defining a wing-shaped formation.

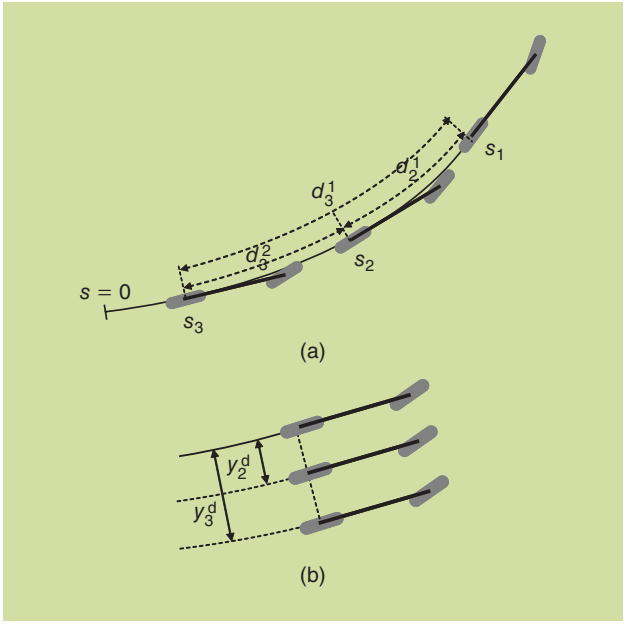

Figure 4. (a) The platoon formation and (b) the line formation.

Another configuration with the set points

$$y_i^d = (i-1)y^* \quad d_i^1 = 0 \quad \forall_i \epsilon \{1, ..., n\}$$

impose that all the robots progress abreast; see Figure 4(b). However, varying set points y_i^d and d_i^k can also be considered, providing a natural way to impose online changes in the formation shape.

The model (1) is attractive since, as any mobile robot kinematic model, it can be converted into a chained form [14]. This feature allows us to address independently lateral and longitudinal control: the two robot control variables, such as the longitudinal velocity v_i at point O_i and the steering angle δ_i, can be designed independently to deal, respectively, with longitudinal and lateral servoing.

For this article to be generic, the situations where fast variations in the robots headings and/or velocities are demanded must be handled. They may be induced by rapid changes in the interactions between the robots and their environment

(such as grip conditions, terrain geometry, and inertial effects), or changes in the shape of the formation to match the application expectations, or just because the reference path exhibits high curvature variations. In such cases, the actuators settling time may decrease the relative positioning accuracy. If several variations are unpredictable (such as changes in leader velocity or in grip conditions), the changes originating from reference path properties can be anticipated to prevent the robots formation from transient mismatches. As a result, both longitudinal and lateral control laws are decomposed into two parts: 1) a reactive part, dealing with unpredictable effects and 2) a predictive part, taking reference trajectory properties (mainly the curvature) into consideration. The two control parts are hereafter detailed.

Because of the adaptive and predictive approaches, highly accurate relative positioning may be obtained.

Reactive Control

Longitudinal Control

The objective of longitudinal control for the ith robot is to maintain a desired curvilinear distance with respect to some other robot within the formation. Depending on the chosen reference robot (1 to n except i), the formation behavior can be slightly different: if the regulation of the ith robot is referred to the immediate preceding $(i-1)$th robot, servoing errors propagation may lead to an oscillating behavior. On the contrary, if the longitudinal errors of all the robots are defined with respect to the first one, there is no servoing errors propagation, but a failure in one of the preceding robots [i.e., the $(i-1)$th robot] can lead to a collision. As a result, to achieve a nonoscillating as well as safe behavior, the longitudinal control of the ith robot with respect to all the other ones is first evaluated and from the collection of $n-1$ velocities v_i^k thus obtained, a mixed control is inferred by means of a linear combination

$$v_i = \sum_{k=1,k\neq i}^{n} \sigma_i^k \, v_i^k \qquad \left(\text{with} \sum_{k=1,k\neq i}^{n} \sigma_i^k = 1\right). \tag{4}$$

The design of the nonlinear longitudinal control law v_i^k when $k=1$ can be found in [18]. The proposed control expression is generalized below to achieve the regulation of the ith robot with respect to the kth one

$$v_i^k = \frac{1-c(s_i)y_i}{\cos(\tilde{\theta}_i+\beta_i^R)}\left(\frac{v_k\cos(\tilde{\theta}_k+\beta_k^R)}{1-c(s_k)y_k}+\kappa_i^k e_i^k+\dot{d}_i^k\right) \tag{5}$$

with κ_i^k, a negative scalar specifying the longitudinal settling time, and $e_i^k = s_i - s_k - d_i^k$ as the longitudinal error of the ith robot with respect to the kth one. Finally, the set of coefficients σ_i^k allows us to specify the expected longitudinal behavior of the formation. These coefficients can be adapted online to modify this behavior or to reflect the communication availability. They also provide a convenient way to shorten or enlarge the formation: σ_i^k is then set to zero or to a nonnull value when the kth robot, leaves or enters the formation, respectively. As a generic control is presented here, the computation or the online modification of these coefficients are not further detailed. It can be computed by a dedicated supervision algorithm, so that the control architecture could fit specific end-user tasks.

Since the sideslip angles β_k^R appear in longitudinal law (4), variations in grip conditions, misestimations in robot parameters or biases in measurements are explicitly taken into account. This allows us to preserve a high level of accuracy in steady-state phases (i.e., slow-varying velocity, curvature, and terrain conditions). Nevertheless, when the reference path or the leader curvature are quickly varying, the velocity of the ith robot has to quickly increase or decrease depending on its lateral deviation. However, due to the actuator settling time, the speed modifications computed by longitudinal law (4) are not applied instantaneously, leading to transient overshoots. The same phenomenon is also encountered in lateral control. A common predictive algorithm, detailed in the "Predictive Control" section, has been developed to address this problem.

Lateral Control

Since the extended kinematic model (1) can be converted into a chained form, lateral control can be designed independently from longitudinal control. The objective can be described as a generalized path tracking task: the ith robot has to follow the reference path Γ, but at some given lateral distance y_i^d. This lateral distance may of course be null [e.g., platoon formation; see Figure 4 (a)], but not necessarily [e.g., wing-shaped or line formations; see Figures 3 or 4(b)], and moreover may also vary in case online reconfiguration of the formation is expected and/or required for safety reasons. More precisely, planned variations in the formation shape (e.g., transition from a wing-shaped formation to a platoon formation to cross a narrow area) can easily be specified by designing y_i^d as a function of s_i. In addition, y_i^d should also depend on the lateral deviations y_k of the immediate neighbors of the ith robot, so that its nominal lateral set point could be immediately altered if one of its neighbors, for any reason, comes abnormally close to it and therefore poses a collision risk. The path following control law designed in [16] is generalized below to meet such requirements, i.e., to allow the tracking of the reference path Γ at some given potentially varying lateral distance y_i^d

$$\delta_i = \arctan\left[\tan\beta_i^R + \frac{l_i}{\cos\beta_i^R}\left(\frac{c(s_i)\cos\gamma_i}{1-c(s_i)y_i} + \frac{A_i\cos^3\gamma_i}{(1-c(s_i)y_i)^2}\right)\right] - \beta_i^F, \tag{6}$$

where

- $\gamma_i = \tilde{\theta}_i + \beta_i^R$
- $A_i = \mu_{i,p}\epsilon_i + (1 - c(s_i)y_i)(\mu_{i,d}(\tan\gamma_i - \dot{y}_i^d / v_i\cos\gamma_i) + c(s_i)\tan^2\gamma_i)$
- $(\mu_{i,p}, \mu_{i,d})$ are negative scalars designing the excepted lateral dynamics
- $\epsilon_i = y_i - y_i^d$ is the lateral error of the ith robot.

The steering law (6) presents exactly the same features as the velocity law (4). On one hand, the effects of poor grip conditions, misestimated parameters, and biased measurements are explicitly accounted in (6) via the online estimated sideslip angles β_i^F and β_i^R, so that highly accurate lateral control can be achieved, at least in steady-state phases. On the other hand, when the reference path curvature or the leader path curvature vary, the steering modifications computed by the lateral law (6) cannot be applied instantaneously because of the actuator settling time, leading to unsatisfactory transient overshoots in lateral error.

Nevertheless, the control law (4), implemented on each robot, constitutes a reactive control framework for potentially varying formations when ideal assumptions with respect to the environment or the robots are not satisfied. It is enhanced in the "Predictive Control" section with a predictive algorithm, to account for the delays induced by both velocity and steering actuators.

Predictive Control

Separation of Control Law Expressions

Fast variations in the reference path or leader curvature result in transient overshoots, since the appropriate velocity and steering values computed from (4) and (6) cannot be applied instantaneously because of the actuators settling time. However the reference path, either supplied beforehand or built online as the leader robot is moving, is always entirely known just ahead of the ith robot. Therefore, its curvature variations can be anticipated and then introduced into control laws (4) and (6) so as to prevent these overshoots.

To reach this objective, the control expressions (5) and (6) are first split into two additive terms: $x_i = x_i^{\text{Dev}} + x_i^{\text{Traj}}$ where x_i stands either for v_i^k or δ_i. The decomposition, detailed in [16] when x_i is the steering angle, is conducted so that each term presents the following features.

- x_i^{Dev} is null when sideslip angles and servoing errors are null. It is therefore a reactive term whose objective is to compensate for guidance errors and unpredictable phenomena. As a result, it cannot benefit from a predictive action and remains unchanged in the sequel.
- x_i^{Traj} is nonnull when servoing errors and sideslip angles are zero. It corresponds roughly to the ideal values of v_i^k or δ_i allowing the ith robot to fulfill its control objective when there is neither sliding nor error. This term relies mainly on the curvature $c(s_i)$ of the reference path at the current location of the ith robot and on its lateral set point y_i^d, and since the future curvature values are known, it can be anticipated.

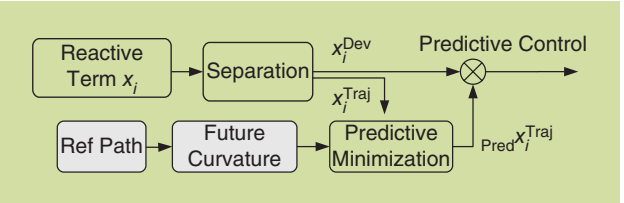

Figure 5. A block diagram of the predictive action.

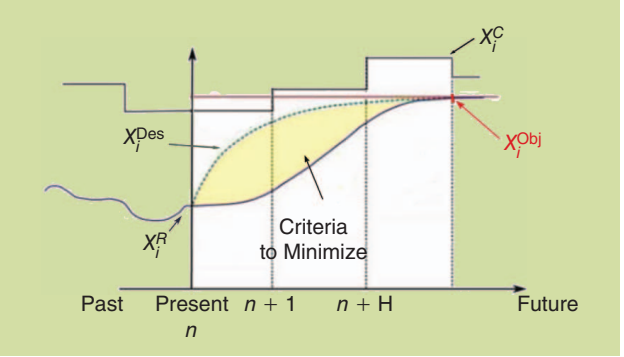

Figure 6. The computation of the predictive term $_{\text{Pred}}x_i^{\text{Traj}}$.

The incorporation of a predictive action into control laws (5) and (6) is then sketched in Figure 5: the reactive term x_i^{Dev} is left unchanged, and the term x_i^{Traj}, relying on the reference path properties (mainly its curvature), is replaced by a term issued from the predictive algorithm, $_{\text{pred}}x_i^{\text{Traj}}$, detailed in the following section. The final control expressions are made up of the previous reactive term and the anticipated one: $x_i = x_i^{\text{Dev}} + {}_{\text{Pred}}x_i^{\text{Traj}}$.

Predictive Control Algorithm

The anticipated term $_{\text{pred}}x_i^{\text{Traj}}$ is derived from the model predictive control principle, see [19].

Beforehand, two models characterizing the responses of the velocity and steering actuators are identified. These models describe the relation between the control values, x_i^C, sent to the actuator and the successive values, x_i^R, of the actuator output. These values can be obtained from a step response.

Next, a temporal horizon H is chosen, with respect to the actuator settling time, and at each control sample period, the location of the ith robot at that horizon is predicted from the robot current velocity and heading. The future curvilinear coordinate s_i^H, as well as the future curvature of the reference path $c(s_i^H)$, are then available, and since x_i^{Traj} depends mainly on $c(s_i)$ and y_i^d, the expected value of x_i^{Traj} at the horizon H can be computed. This computation also constitutes a reasonable estimation of the value the actuator output should be taken at the horizon H, and is therefore denoted x_i^{Obj}. A temporal desired behavior bringing x_i^R from its current value to x_i^{Obj} is then built (see Figure 6) and a minimization algorithm relying on the actuator model is applied to find the control sequence x_i^C on the horizon H so that the actuator output x_i^R best follows this desired behavior.

The predictive term ${}_{\text{Pred}}x_i^{\text{Traj}}$ is then defined as the first term of the sequence x_i^C previously obtained, since it is the control value that should be sent to the actuator at the current time, in order for its output x_i^R to reach the expected value x_i^{Obj} at the horizon H. The computation of x_i^{Obj} and the associated minimization are then repeated at each subsequent control sample period. Eventually, the final control expressions result in the addition of the reactive term x_i^{Dev} designed to reject unpredictable errors and the predictive term ${}_{\text{Pred}}x_i^{\text{Traj}}$ (see Figure 5) designed to anticipate the curvature variations and reduce transient overshoots due to actuators settling time.

Summary of the Formation Control Framework

The proposed framework for formation control is composed of several layers addressing different phenomena. The overall control scheme for the ith robot in a formation constituted of n robots is shown in Figure 7.

The reference path in the top left part in Figure 7 is either supplied beforehand or inferred online from the motion of the leader robot and constitutes a common reference. The relative positions of the robots with respect to this path are then compared with the desired ones and the longitudinal and lateral errors obtained are sent to the control laws.

These control laws are designed from an extended kinematic model, adapted online by means of an observer, which ensures the convergence of the model outputs to the corresponding measured variables, and consequently the online representativeness of the model. The structural properties of the extended kinematic model are nevertheless similar to those of more conventional kinematic models of mobile robots; in particular, it can be converted into a chained form, so that longitudinal and lateral controls can actually be designed independently.

Both control laws consist of two terms: 1) a reactive term dealing with unpredictable events (such as changes in grip conditions) and 2) a predictive term whose objective is to anticipate variations in curvature (by considering the reference path just ahead of the robot), to avoid transient overshoots due to the actuators settling time. Eventually, the $n-1$ longitudinal laws computed for the ith robot, considering the other robots as a reference, are gathered by means of a linear combination. The combination coefficients may be changed online to modify either the formation behavior or the number of robots involved in the formation. The velocity and steering angle values obtained are then sent to the actuators of the ith robot, whose settling times have been taken into account by the predictive terms. Accurate control of a potentially varying formation can then be achieved, whatever the interactions between the robots and the environment and whatever the properties of the actuators.

This general control scheme supposes a bidirectional communication between all the robots, which is not necessarily ensured permanently. Nevertheless, the coefficients of the linear combination of the elementary longitudinal laws or the weights on the lateral deviations of the other robots within the desired lateral deviation of the ith robot can be modified online to react to the current communication availability. More generally, the different layers of the proposed control framework can be configured to fit with the application context: if sliding effects are negligible, the model adaptation can easily be omitted by simply freezing the sideslip angle values to zero. In the same way, if the actuators settling times can be neglected, then the prediction algorithm can be omitted by setting the prediction horizon H to zero. In these cases, the proposed control laws are just brought back to the ones proposed for the ideal case (motion without sliding and ideal actuators) from which they have been derived.

Simulation Results

To validate the multirobots coordination and the mixed control, simulations have been realized. In the scenario considered, five robots are tracking the trajectory presented in Figure 8. It is 100 m long and composed of two turns at abscissa 18 and 57 m (respectively on the left and right) linked by straight lines. The robots are moving in a so-called kite configuration, a mix of a wing-shaped formation (for robots 1, 2, and 3) and a platoon formation (for robots 1, 4, and 5). The desired positions of the robots, i.e., their lateral distance to the trajectory and longitudinal distance to the first robot, are detailed in Table 1.

In their initial positions, the robots are all side-by-side at the abscissa $s = 0$ m, at a lateral distance of 2 m from each other. The robots behavior is

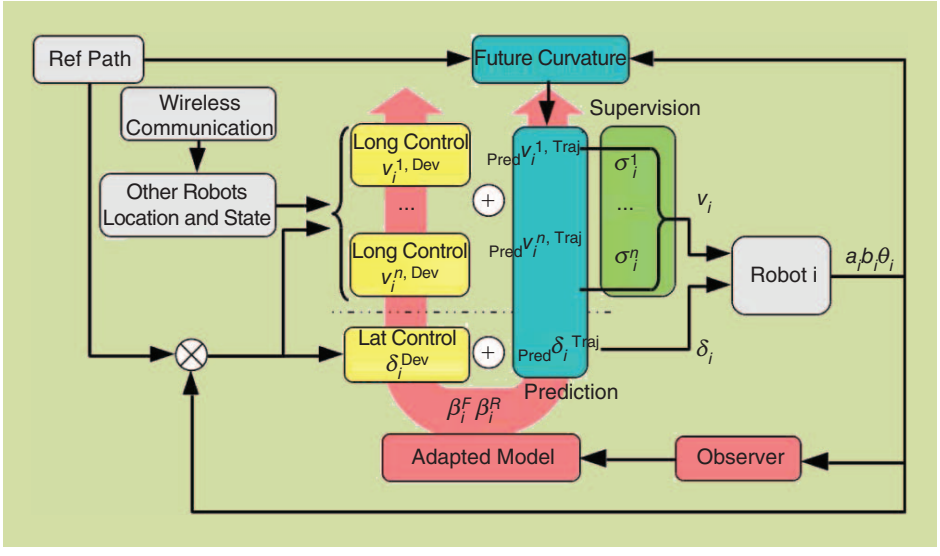

Figure 7. The overall formation control framework.

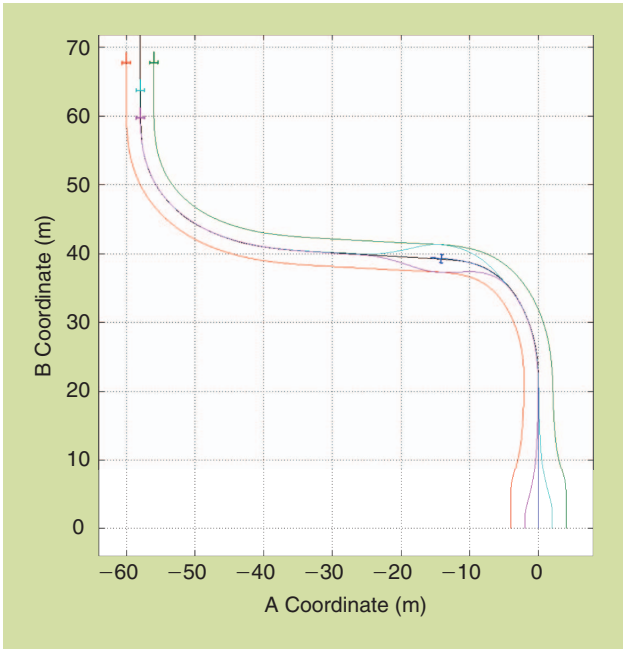

Figure 8. The reference and trajectories of the robots.

simulated with a dynamic model and the actuators are modeled as second-order systems with a settling time of 0.7 s.

The leader, robot 1, travels at a constant velocity of 3 m/s and the follower robots are referenced to the leader for the longitudinal control, i.e., $\sigma_i^1 = 1$ in the longitudinal control law (4). At the abscissa 40 m, a failure of the leader is simulated, so the robot 1 stops and sends a fault message to the follower robots. The situation being potentially hazardous, the combination parameters σ_i^k are then adapted to $\sigma_i^{i-1} = 1$, so that the robots are referenced to the preceding one. As the first robot is removed from the fleet, the velocity of the second robot is then set to 3 m/s so that the formation still progresses along the reference path. In the mean time, to avoid the stationary robot and keep safe distances from one another, robots 4 and 5 desired distances are recalculated. First, a sinusoidal avoidance trajectory is defined around the position of the first robot (y_4^d and y_5^d vary from 0 to 2 m and from 0 to −2 m, respectively). Next, as their desired lateral deviation brings robots 4 and 5 behind robots 2 and 3, their interdistance is linearly increased up to two more meters, before coming back to their initial distances when the stationary robot is passed.

Figures 9 and 10 present the lateral and longitudinal results of the path tracking with respect to the curvilinear abscissa of the robots. Initially, the vehicles are positioned abreast so the leader starts first and the other robots start moving when their desired interdistance is attained. In the first simulation, shown in Figure 9, the adaptive control laws (5) and (6) have been used without the predictive overlay. From the initial positions, all robots converge to the desired formation shape, albeit with an overshoot of 0.6 m on the longitudinal side due to the settling time of the actuators. However, from the moment the desired positions vary, as

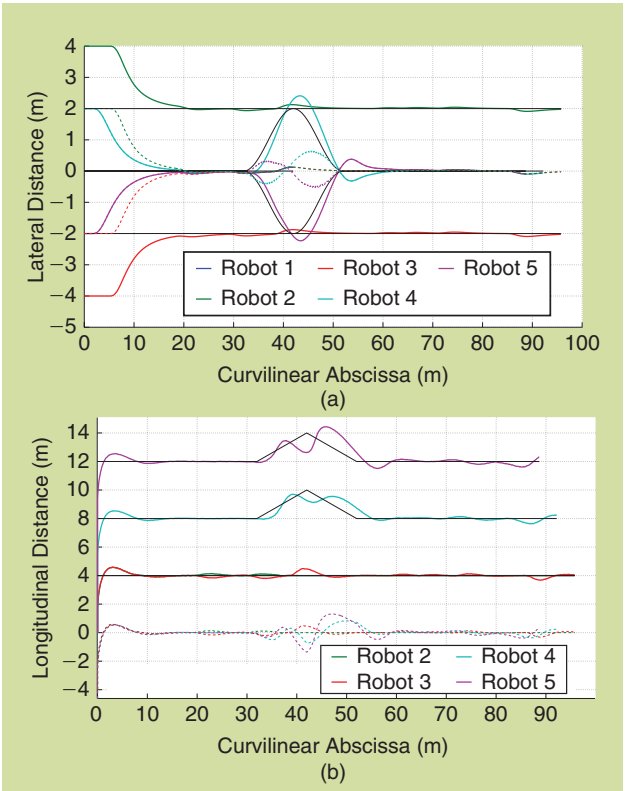

Figure 9. The tracking results without prediction: (a) lateral distances to the trajectory and errors (dashed lines) and (b) curvilinear distances and errors to the leader (dashed lines).

the control laws account for the current desired positions only, tracking errors appear due to the actuators settling time. Moreover, for the longitudinal servoing, since the reference robot is now the preceding one, the positioning errors are accumulated and amplified from the head (robot 2) to the tail (robot 5) of the formation, as seen in dashed lines in Figure 9(b).

A reactive term whose objective is to compensate for guidance errors.

In the second simulation, the predictive part described in the "Predictive Control" section has been added and the results are shown in Figure 10. The prediction takes into account the future curvature of the reference path as well as the variations in the desired position so that the tracking errors are suppressed. It should also be noted that when robot 1 stops at $s = 40$ m (robots 2 and 3 are at $s = 36$ m, robot 4 at $s = 32$ m, and robot 5 at $s = 28$ m) the referencing is

Table 1. Parameters of the desired formation.

Robots	1	2	3	4	5
y_i^d	0 m	2 m	−2 m	0 m	0 m
d_i^1		4 m	4 m	8 m	12 m

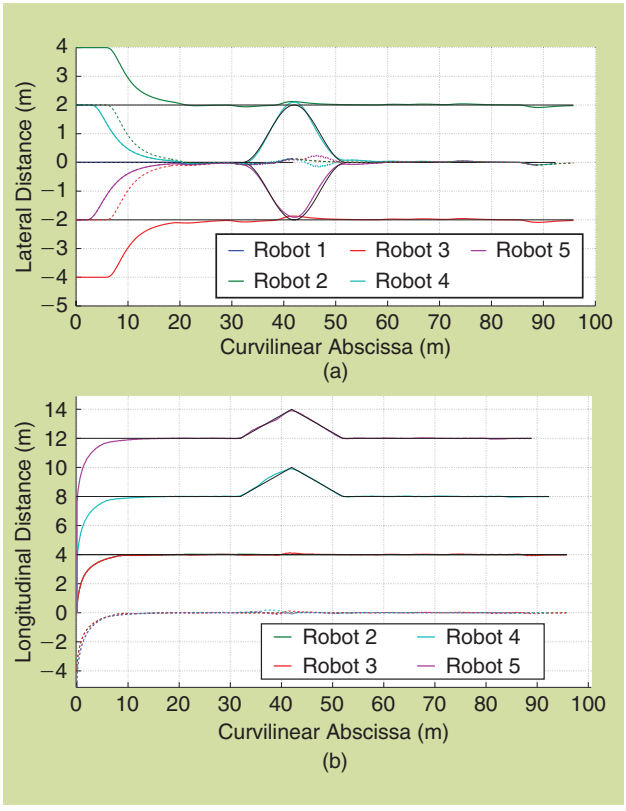

Figure 10. The tracking results with prediction: (a) lateral distances to the trajectory and errors (dashed lines) and (b) curvilinear distances and errors to the leader (dashed lines).

Figure 11. The off-road robots in formation with RobuFAST leading Arocco.

Table 2. Main properties of the mobile robots.

Robots	RobuFAST	Arocco
Total mass	420 kg	620 kg
Wheelbase	1.2 m	1.2 m
Maximum speed	8 m/s	3.5 m/s
Wheel width	5 cm	15 cm
Driving motors settling time	1.0 s	1.5 s
Steering motors settling time	0.4 s	0.6 s

transferred to the previous robot, and the accuracy of the tracking is maintained, with maximal errors of 20 cm and 30 cm for the lateral and the longitudinal parts, respectively. An animation of the simulated path tracking is available at ftp://ftp.clermont.cemagref.fr/TSCF/AudreyGuillet/RAM/.

Experimental Results

Experimental Testbed

The capabilities of the proposed approach have also been investigated by means of full scale experiments conducted with the mobile robots RobuFAST and Arocco shown in Figure 11.

These off-road mobile robots are electric vehicles with four independent motors. They are specifically designed for mobility in the natural environment, for instance longitudinal slopes up to 45° can be passed. They share a similar chassis, but their main characteristics are quite different; see Table 2. Therefore, the robot-related parameters of the control laws (mass, prediction time, and low-level behavior) are adapted for each robot to their characteristics. In contrast, the high-level control law settings (observer parameters and convergence gains) are the same for all the robots, to impose a consistent behavior to the formation.

To acquire the robots absolute localization, required in observer equations (3) as well as in velocity and steering control laws (5) and (6), a real-time kinematic global positioning system (RTK-GPS) receiver is installed onboard. It supplies an absolute position accurate to within 2 cm, at a 10-Hz sampling frequency. The GPS antenna is settled to the middle of the rear axle, so that the location of O_i (i.e., the point to be controlled; see Figure 2) is obtained directly from the sensor.

To implement formation control, a wireless local area network (WLAN) is set up for the exchange of localization data between the robots. The data are timestamped prior to being sent and resampled before their use in formation control laws, so that the computed longitudinal and lateral errors are always temporally consistent.

Results in Off-Road Conditions

Two sets of experiments have been conducted in a natural environment context to demonstrate the performances of the proposed control framework when both the ground conditions and the formation shape are varying.

In the first set of experiments, path tracking with respect to the path depicted in black line in Figure 12 has been considered. This path has been recorded beforehand, when the robot was steered manually at 1 m/s. It is composed of an initial straight line, a 90° turn on the right followed by two sharp turns on the left, and a final straight line. Since the robots operate off-road and grip conditions are varying (alternating between grass and asphalt), the adaptive and predictive layers of the proposed control framework are used.

Two path trackings have been realized in the wing-shaped formation with different desired distances. In both cases, the leader robot follows the path at a constant speed of 2 m/s and the desired interdistance is $d^* = 9$ m. As for the desired lateral

distance, in the first case $y^* = -3$ m, so that the follower robot is inside the curve, and in the second case $y^* = 2$ m so that it is on the outside of the main curve. The results of the follower positioning in both path trackings are presented in Figure 13.

In the first path tracking, the follower is at the inside of the curve, and since the curvature of the reference path is high at the abscissa $s = 50$ m, it is near the instantaneous center of rotation at that location and almost has to stop to keep the desired interdistance, leading to some transient lateral and longitudinal tracking errors (see the blue line in Figure 13). During the second path tracking, the follower robot is at the exterior of the main curve. Therefore, when the curvature of the path increases sharply (still at $s = 50$ m), the robot has to accelerate quickly to keep the formation. Given the low-level limitations, a transient longitudinal error appears, but is quickly eliminated when the robot reaches the required velocity. Overall, even with those physical limitations, the formation servoing ensures a satisfactory accuracy, with a standard deviation of 0.15 m for the lateral control and 0.4 m for the longitudinal positioning.

In the second experiment, the two off-road robots RobuFAST and Arocco (see Figure 11) must execute autonomously the mission illustrated in Figure 14: they should operate in a wing-shaped formation (see Figure 3) except during the half-turn where the desired formation shape is the platoon formation. The terrain consists of grass, except during the half-turn executed on asphalt. The velocity of the first vehicle is 2 m/s, the desired interdistance is $d^* = 9$ m (in both formation shapes) and the desired lateral deviation in wing-shaped formation is $y^* = -2$ m.

The actual trajectories of RobuFAST (leader robot) and Arocco (follower) shown in blue and red, respectively, in Figure 14, show that the mission objectives, with the changes in the formation shape, have been achieved. For further analysis, the lateral deviations of the two robots with respect to the reference path are reported in Figure 15(a). We observe that the changes in the formation shape are executed smoothly: y_2 varies from -2 to 0 m and from 0 to -2 m without any overshoot. It can also be observed that high lateral guidance accuracy is achieved in the parts where the formation shape is unchanged: lateral errors never exceed 10 cm, despite poor grip conditions (when the robots move on grass) and sharp curves (during the half-turn). This demonstrates the relevance of the adaptive and predictive layers of the proposed control framework.

Finally, performances of the longitudinal control law are investigated. The velocity of the leader robot is constant. In contrast, the velocity of the follower is supposed to vary in order to maintain the desired interdistance despite the changes in the formation shape, the sharp curves, or simply the contact conditions. The curvilinear distance between the two robots is shown in blue in Figure 15(b). It can be observed that after initialization, the longitudinal error never exceeds 15 cm and even when the formation configuration is changed, the longitudinal control law achieves a null error.

Videos of the experimental path trackings can be found at ftp://ftp.clermont.cemagref.fr/TSCF/AudreyGuillet/RAM/. Other experimental results demonstrating the relevance of the adaptive and predictive layers of the proposed control framework with respect to harsh grip conditions or different terrain geometry (sloping ground) or actuator

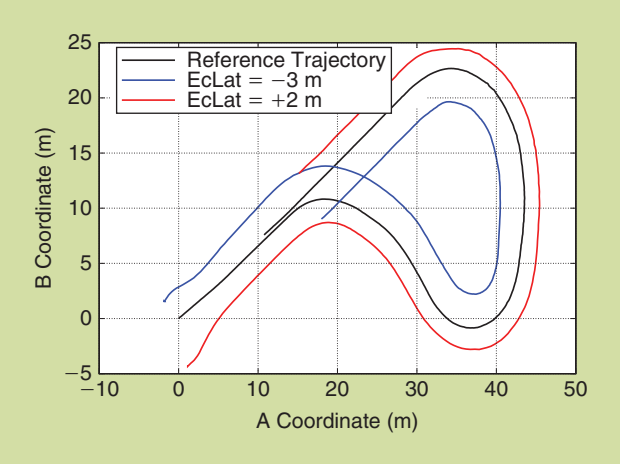

Figure 12. The reference path and trajectories achieved in the two configurations.

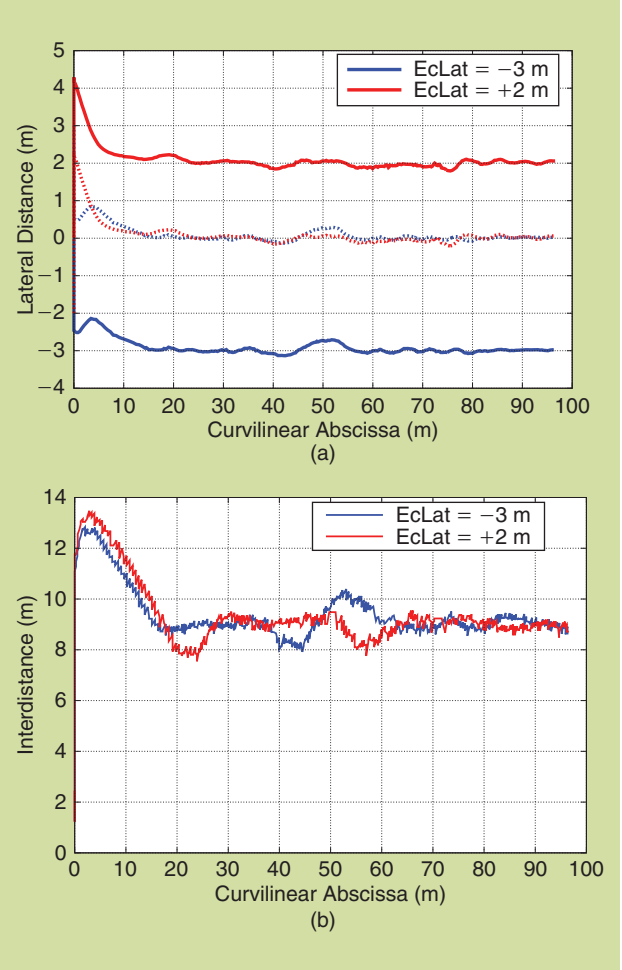

Figure 13. The path tracking results in the two configurations: (a) lateral distances and errors of the follower (dashed lines) and (b) curvilinear interdistance between the leader and the follower.

dynamics can be found in [17]. The same control framework has also been successfully implemented to achieve accurate platooning with small urban electric vehicles intended for the ultimate short displacements within a multimodal transportation system. An identical level of accuracy has been demonstrated, although monocular cameras have been considered, instead of RTK GPS sensors, to ensure a reliable vehicle localization in the urban environment, see [20].

Conclusions and Future Work

This article proposes a generic formation control framework enabling accurate relative positioning in various multirobots applications. Based on a path tracking approach, adaptive and predictive control have been developed to supplement the standard longitudinal and lateral control laws proposed for ideal robots satisfying pure rolling without sliding assumptions, so that guidance accuracy can be preserved whatever the grip conditions, terrain geometry, misestimated robot parameters, biased measurements or actuators settling time. In addition, the proposed approach allows us to address the control of any formation shape, as well as online formation shape modification or addition/withdrawal of robots. The performances have been largely investigated by means of numerous full-scale experiments carried out in off-road environments. The proposed approach is generic and open and permits us to address various formation control applications in order to meet end-users expectations.

To develop the capabilities of this approach further, three axes may be considered. First, the accuracy of control laws can still be improved by extending the scope of the predictive action. Currently, only the variations in the reference path curvature are anticipated. Higher control accuracy could be achieved if the upcoming changes in the terrain geometry and in the contact conditions could also be taken into account. However, it is difficult to acquire relevant information to be reported into the predictive algorithm. If each robot, for the needs of a specific application, is equipped with an elaborate sensing device supplying it with a local digital elevation map online (for instance, a stereovision system), then terrain information could be extracted from it. Otherwise, the main terrain features could be inferred from the sideslip angles and the cornering stiffnesses estimated by each robot. If they are sent jointly with the localization data to the other robots via wireless communication, the robots located behind could then incorporate this information into the predictive algorithm to anticipate the major terrain variations (such as a transition from grass to asphalt) and the transient longitudinal and lateral errors due to the actuators settling time could be reduced.

Next, the control law accuracy is not the only performance index to be considered: safety of the robot must also

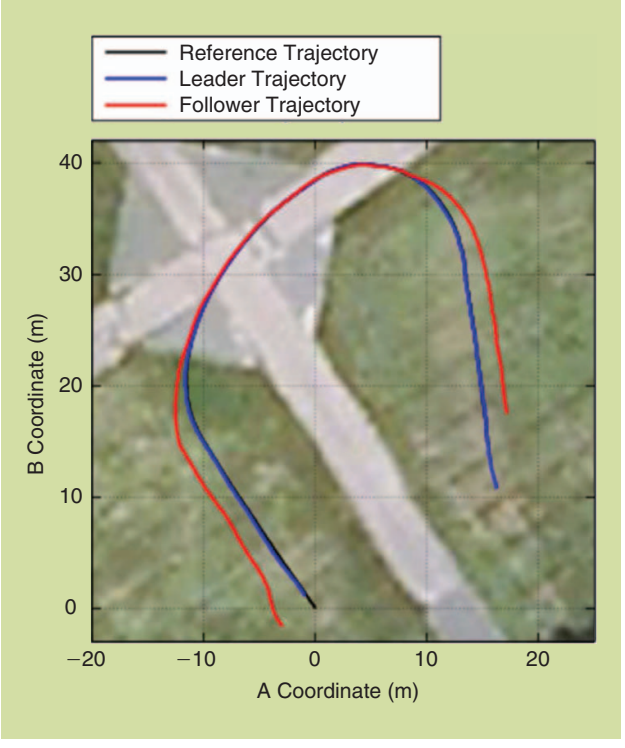

Figure 14. The reference path and trajectories achieved.

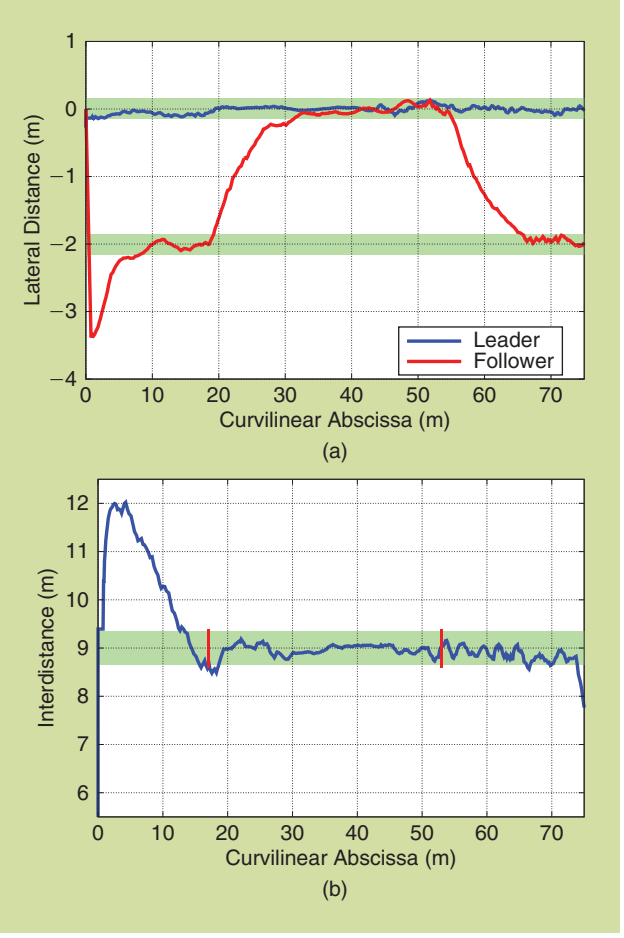

Figure 15. The results of the path tracking with variable desired lateral distance: (a) lateral deviations of the leader (blue) and of the follower (red) and (b) curvilinear interdistance between the leader and the follower.

be permanently ensured. In off-road situations, both terrain geometry and contact conditions may lead the robots to hazardous situations that might result in either a fatal rollover crash or a loss of controllability if the values delivered by the control laws exceed the actuators limits. In the latter case, the robot may deviate from its expected trajectory or even spin around. To protect each robot from hazardous situations, these scenarios should first be quantified by some metrics (for instance, the lateral load transfer metrics can be used to evaluate the rollover risk). Since robot dynamic stability is investigated, mixed kinematic and dynamic models have to be developed to enable both estimation and prediction of these metrics. Next, predictive control approaches can be considered to compute the control values at each sampling period that would lead to a hazardous situation within a short time window. If the values supplied by the guidance control laws were exceeding these limit values, then they could be instantaneously overwritten so that the robots could be preserved from any severe risk.

Finally, only standard scenarios have been considered when designing the longitudinal coefficients σ_i^k and the lateral set point functions y_k^d (transition from one formation shape to another one, basic security procedures in presence of obstacles, short communication losses, and addition/withdrawal of a robot). For the formation supervisor to meet any specific application requirements, more general scenarios have to also be addressed. To ensure that a consistent and safe behavior is maintained despite the scenario complexity, general frameworks such as graph theory should be explored for the design of these coefficients/functions.

Acknowledgments

This work has been sponsored by the French government research program Investissements d'Avenir through the RobotEx Equipment of Excellence (ANR-10-EQPX-44) and the IMobS3 Laboratory of Excellence (ANR-10-LABX-16-01), by the European Union through the program Regional Competitiveness and Employment 2007–2013 (ERDF Auvergne region), by the Auvergne region, and by the French Institute for Advanced Mechanics.

References

[1] M. Buehler, K. Iagnemma, and S. Sanjiv, "The 2005 DARPA Grand Challenge: The great robot race," in *Springer Tracts in Advanced Robotics*, vol. 36. Berlin: Springer-Verlag, 2007.

[2] M. Montemerlo, J. Becker, S. Bhat, H. Dahlkamp, D. Dolgov, S. Ettinger, D. Haehnel, T. Hilden, G. Hoffmann, B. Huhnke, D. Johnston, S. Klumpp, D. Langer, A. Levandowski, J. Levinson, J. Marcil, D. Orenstein, J. Paefgen, I. Penny, A. Petrovskaya, M. Pflueger, G. Stanek, D. Stavens, A. Vogt, and S. Thrun, "Junior: The Stanford entry in the urban challenge," *J. Field Robot.*, vol. 25, no. 9, pp. 569–597, 2008.

[3] J. Levinson, J. Askeland, J. Becker, J. Dolson, D. Held, S. Kammel, J. Kolter, D. Langer, O. Pink, V. Pratt, M. Sokolsky, G. Stanek, D. Stavens, A. Teichman, M. Werling, and S. Thrun, "Towards fully autonomous driving: Systems and algorithms," in *Proc. Intelligent Vehicles Symp. (IV)*, 2011, pp. 163–168.

[4] R. Bishop, "Intelligent vehicle applications worldwide," *IEEE Intell. Syst.*, vol. 15, no. 1, pp. 78–81, Jan./Feb. 2000.

[5] P. Petrov, "A mathematical model for control of an autonomous vehicle convoy," *Trans. syst. control*, vol. 3, no. 9, pp. 835–848, 2008.

[6] S. Blackmore, B. Stout, M. Wang, and B. Runov, "Robotic agriculture—the future of agricultural mechanisation?" in *Proc. 5th European Conf. Precision Agriculture*, Upsala, Sweden, 2005, pp. 621–628.

[7] E. Sahin, "Swarm robotics: From sources of inspiration to domains of application," in *Swarm Robotics, Proceedings of the SAB 2004 International Workshop* (Lecture Notes in Computer Science). Berlin, Heidelberg: Springer, 2004.

[8] G. Antonelli, F. Arrichiello, F. Caccavale, and A. Marino, "Decentralized centroid and formation control for multi-robot systems," in *IEEE Int. Conf. Robotics Automation*, Karlsruhe, Germany, 2013, pp. 3511–3516.

[9] T. Liu and Z. Jiang, "Distributed formation control of nonholonomic mobile robots without global position measurements," *Automatica*, vol. 49, no. 2, pp. 592–600, 2013.

[10] S. Pedersen, S. Fountas, H. Have, and B. Blackmore, "Agricultural robots–system analysis and economic feasibility," *Precis. Agriculture*, vol. 7, no. 4, pp. 295–308, 2006.

[11] N. Noguchi, J. Will, J. Reid, and Q. Zhang, "Development of a master-slave robot system for farm operations," *Computers Electron. Agriculture*, vol. 44, no. 1, pp. 1–19, 2004.

[12] X. Zhang, M. Geimer, P. Noack, and L. Grandl, "A semi-autonomous tractor in an intelligent master—slave vehicle system," *Intell. Service Robot.*, vol. 3, no. 4, pp. 263–269, 2010.

[13] H. Yamaguchi, T. Arai, and G. Beni, "A distributed control scheme for multiple robotic vehicles to make group formations," *Robot. Auton. Syst.*, vol. 36, no. 4, pp. 125–147, 2001.

[14] C. Samson, "Control of chained systems application to path following and time-varying point stabilization of mobile robots," *IEEE Trans. Autom. Contr.*, vol. 40, no. 1, pp. 64–77, 1995.

[15] F. Ben Amar and P. Bidaud, "Dynamic analysis of off-road vehicles," in *Proc. Int. Symp. Experimental Robotics*, Stanford, 1995, pp. 363–371.

[16] R. Lenain, B. Thuilot, C. Cariou, and P. Martinet, "High accuracy path tracking for vehicles in presence of sliding: Application to farm vehicle automatic guidance for agricultural tasks," *Auton. Robot.*, vol. 21, no. 1, pp. 79–97, 2006.

[17] C. Cariou, R. Lenain, B. Thuilot, and M. Berducat, "Automatic guidance of a four-wheel-steering mobile robot for accurate field operations," *J. Field Robot.*, vol. 26, nos. 6–7, pp. 504–518, 2009.

[18] J. Bom, B. Thuilot, F. Marmoiton, and P. Martinet, "A global control strategy for urban vehicles platooning relying on nonlinear decoupling laws," in *IEEE/RSJ Int. Conf. Intelligent Robots Systems*, 2005, pp. 2875–2880.

[19] J. Richalet, "Industrial applications of model based predictive control," *Automatica*, vol. 29, no. 5, pp. 1251–1274, 1993.

[20] P. Avanzini, E. Royer, B. Thuilot, and J.-P. Dérutin, "Using monocular visual SLAM to manually convoy a fleet of automatic urban vehicles," in *Proc. IEEE Int. Conf. Robotics Automation*, Karlsruhe, Germany, 2013, pp. 3219– 3224.

Audrey Guillet, Irstea, Clermont-Ferrand, France. E-mail: audrey.guillet@irstea.fr.

Roland Lenain, Irstea, Cleront-Ferrand, France. E-mail: roland.lenain@irstea.fr.

Benoit Thuilot, Institut Pascal (CNRS—UMR 6602), Clermont-Ferrand University, France. E-mail: benoit.thuilot@univ-bpclermont.fr.

Philippe Martinet, IRCCYN (CNRS—UMR 6597), École Centrale de Nantes, France. E-mail: philippe.martinet@irccyn.ec-nantes.fr.